The Journal of Chemical Physics

Detection and characterization of the tin dihydride (SnH_2 and SnD_2) molecule in the gas phase

Cite as: J. Chem. Phys. **148**, 024302 (2018); https://doi.org/10.1063/1.5011162
Submitted: 30 October 2017 . Accepted: 18 December 2017 . Published Online: 09 January 2018

Tony C. Smith, and Dennis J. Clouthier

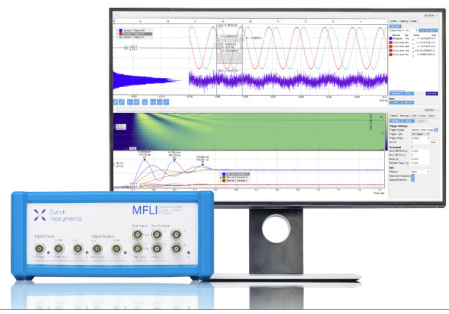

Detection and characterization of the tin dihydride (SnH_2 and SnD_2) molecule in the gas phase

Tony C. Smith[1] and Dennis J. Clouthier[2,a)]
[1]*Ideal Vacuum Products, LLC, 5910 Midway Park Blvd. NE, Albuquerque, New Mexico 87109, USA*
[2]*Department of Chemistry, University of Kentucky, Lexington, Kentucky 40506–0055, USA*

(Received 30 October 2017; accepted 18 December 2017; published online 9 January 2018)

The SnH_2 and SnD_2 molecules have been detected for the first time in the gas phase by laser-induced fluorescence (LIF) and emission spectroscopic techniques through the $\tilde{A}^1B_1$–$\tilde{X}^1A_1$ electronic transition. These reactive species were prepared in a pulsed electric discharge jet using $(CH_3)_4Sn$ or SnH_4/SnD_4 precursors diluted in high pressure argon. Transitions to the electronic excited state of the jet-cooled molecules were probed with LIF, and the ground state energy levels were measured from single rovibronic level emission spectra. The LIF spectrum of SnD_2 afforded sufficient rotational structure to determine the ground and excited state geometries: $r_0'' = 1.768$ Å, $\theta_0'' = 91.0°$, $r_0' = 1.729$ Å, $\theta_0' = 122.9°$. All of the observed LIF bands show evidence of a rotational-level-dependent predissociation process which rapidly decreases the fluorescence yield and lifetime with increasing rotational angular momentum in each excited vibronic level. This behavior is analogous to that observed in SiH_2 and GeH_2 and is suggested to lead to the formation of ground state tin atoms and hydrogen molecules. *Published by AIP Publishing.* https://doi.org/10.1063/1.5011162

I. INTRODUCTION

Tin compounds have found extensive use in organic synthesis.[1,2] They are also industrially important in the production of tin-containing thin films, oxides, and heterostructures. Typical precursors for the practical chemical vapor deposition (CVD) of tin oxide are tin tetrachloride ($SnCl_4$), dimethyltin dichloride [$(CH_3)_2SnCl_2$], and monobutyltin trichloride [n-$C_4H_9SnCl_3$].[3,4] In a recent review[3] of the gas-phase thermochemistry and mechanism of organometallic tin oxide CVD precursors, Allendorf and van Mol concluded that "lack of data concerning both the thermochemistry and kinetics of these reactions inhibits the development of predictive models that can be used for process optimization." This lack of fundamental data and the dearth of previous spectroscopic investigations stimulated our interest in small tin-containing reactive intermediates.

In recent years, tin-containing heterostructures such as Ge–Sn and Si–Ge–Sn have attracted a lot of attention due to the possibility of their extending and enhancing the properties of basic silicon devices.[5–7] Most of the recent work in this area has involved CVD growth of thin films on silicon or germanium substrates with stannane (SnH_4 or SnD_4) and germanium hydride (GeH_4, Ge_2H_6, or Ge_3H_8) feed gases. Our review of the literature showed that even the very simplest polyatomic tin-containing species, tin dihydride, was unknown in the gas phase despite its likely intermediacy in such CVD processes.

The lighter group IV dihydrides are well known. Methylene (CH_2), with a triplet ($\tilde{X}^3B_1$) ground state, is the odd man out, as silylene (SiH_2) and germylene (GeH_2) both have all their electrons paired up ($\tilde{X}^1A_1$) in the ground state. This is because the 2*s* and 2*p* orbitals of carbon are very close in energy, hybridization readily occurs (as evidenced by the CH_2 bond angle of ~134°),[8] and the resulting $s\sigma$ and $p\pi$ orbitals are almost degenerate, so formation of the triplet state avoids the energetic cost of spin pairing (singlet-triplet splitting of ~3156 cm^{-1}). By contrast, the heavy carbene analogs involve *s* and *p* valence orbitals of quite different energies, hybridization does not occur (the ground state bond angles are all near 90°),[9] and the $s\sigma$ (a_1) and $p\pi$ (b_1) orbitals are much further apart (singlet-triplet splittings of ~8000 cm^{-1}). Both silylene and germylene are known to undergo a rotational-level-dependent predissociation in the first singlet excited electronic state which leads to production of hydrogen molecules and silicon or germanium atoms.[10,11] For this reason, the $\tilde{A}^1B_1$–$\tilde{X}^1A_1$ laser induced fluorescence (LIF) spectra of SiH_2 and GeH_2 exhibit a very limited number of rotational lines, terminating on the very lowest rotational energy levels in the excited state. The predissociation leads to rapidly decreasing fluorescence lifetimes in higher rotational states and marginal quantum yields of fluorescence.

The known properties of stannylene (SnH_2) come from a single infrared matrix study[12] and a few theoretical investigations. In 2002, the Lester Andrews group laser-ablated a tin rod and codeposited it with H_2 or D_2 in argon and observed SnH_2/SnD_2 antisymmetric stretching (ν_3) bands at 1681.8/1200.7 cm^{-1}. There is no further experimental data available for tin dihydride.

In 1986, Balasubramanian[13] reported complete active space self-consistent field/configuration interaction (CAS SCF/CI) calculations on the ground and first two excited states of SnH_2. Relativistic effects from the tin atom were estimated

a)Author to whom correspondence should be addressed: dclaser@uky.edu.

through the use of effective core potentials. The author found that SnH_2 is bent in the $\tilde{X}^1A_1$ [r(SnH) = 1.780 Å, θ = 91.6°], $\tilde{a}^3B_1$ [r(SnH) = 1.719 Å, θ = 118.8°, ΔE = 22.5 kcal/mol] and $\tilde{A}^1B_1$ [r(SnH) = 1.754 Å, θ = 119.9°, ΔE = 48.5 kcal/mol] states and that the spectroscopically accessible $\tilde{A}$ state should occur at about 17 000 cm^{-1}. Subsequent studies of the SnH_2 ground state gave similar geometric parameters.[14,15] Finally, in 1996, Gordon and co-workers[16] calculated relativistic potential energy surfaces for the $\tilde{X}$ and $\tilde{a}$ states of SnH_2 and obtained ground state vibrational frequencies of ν_1 = 1627.3, ν_2 = 792.5, and ν_3 = 1627.4 cm^{-1}, a singlet–triplet gap of 23.7 kcal/mol, and an intersystem crossing probability of essentially unity.

In the present work, we have produced SnH_2 and SnD_2 in the gas phase in a supersonic expansion discharge jet and detected it by laser induced fluorescence through the $\tilde{A}^1B_1$–$\tilde{X}^1A_1$ electronic transition. Sufficient data have been obtained to determine the ground and excited state geometries of tin dihydride, and some of the vibrational frequencies in the combining states have been measured by LIF and emission spectroscopy. The LIF spectra and measured single rotational level fluorescence lifetimes show that SnH_2 undergoes a rotational-level-dependent predissociation in the excited state. Precise transition frequencies by which the reactive intermediate can be monitored by absorption or LIF methods have been measured.

II. EXPERIMENT

The SnH_2 or SnD_2 reactive intermediates were generated by seeding the vapor of a suitable tin-containing precursor into high pressure argon and subjecting pulses of this gas mixture to an electric discharge. As described in detail elsewhere,[17,18] a pulsed molecular beam valve (General Valve, series 9) injected the precursor mixture into a flow channel where an electric discharge between two stainless steel ring electrodes fragmented the precursor, producing tin dihydride and a variety of other products. The reactive intermediates were rotationally and vibrationally cooled by free jet expansion into vacuum at the exit of the pulsed discharge apparatus. A 1.0 cm long reheat tube[19] added to the end of the discharge channel increased production of the species of interest and suppressed the background glow from excited argon atoms.

Moderate resolution (0.1 cm^{-1}) survey LIF spectra were recorded using a neodymium: yttrium aluminum garnet (Nd:YAG) pumped dye laser (Lumonics HD-500) excitation source. The fluorescence was collected by a lens and focused through appropriate longwave pass filters onto the photocathode of a photomultiplier tube (RCA C31034A). The spectra were calibrated with optogalvanic lines from various argon- and neon-filled hollow cathode lamps to an estimated absolute accuracy of 0.1 cm^{-1}. The laser-induced fluorescence and calibration spectra were digitized and recorded simultaneously on a homebuilt computerized data acquisition system.

Higher resolution (0.035 cm^{-1}) LIF spectra were obtained in the same apparatus using a Lambda Physik Scanmate 2E dye laser, with an angle-tuned etalon inserted in the cavity of the laser. The spectra were calibrated to an estimated accuracy of 0.005 cm^{-1} using I_2 LIF lines.[20]

For emission spectroscopy, previously measured LIF band maxima in the spectra of SnH_2 or SnD_2 were excited by the dye laser and the resulting fluorescence was collected with an f/0.7 aspheric lens and imaged with f/4 optics onto the entrance slit of a 0.5 m scanning monochromator (Spex 500M). The pulsed fluorescence signals were detected with a gated CCD camera (Andor iStar 320T with 18 mm effective active area) and recorded digitally. The emission spectra were calibrated to an estimated accuracy of ±1 cm^{-1} using emission lines from a neon lamp. A 1200 line/mm grating blazed at 750 nm was employed in this work, which gave a bandpass of 29.9 nm with 18 mm effective active area on the CCD. A spectral resolution of 0.2 nm was typical, depending on the signal intensity.

Fluorescence lifetimes were measured by summation averaging 500 fluorescence decay curves employing a Tektronix TDS-3054 oscilloscope, with the excitation laser tuned to a single rotational LIF line. The laser was then slightly detuned from the LIF line, a second background sum was recorded, and it was subtracted from the fluorescence decay curve to remove the scattered laser light and discharge glow contributions. The resulting data were plotted as the natural log of the fluorescence intensity versus time, and the linear portion of the decay was least squares fitted to a straight line to obtain the fluorescence lifetime and statistical error.

Tetramethyltin (Aldrich, 95%), as received, was poured into a Pyrex U-tube, degassed, and pressurized with 40–60 psi of argon, and the mixture was used as a SnH_2 precursor. Stannane (SnH_4) and fully deuterated stannane (SnD_4) were synthesized by the low temperature reduction of $SnCl_4$ with $LiAlH_4$/$LiAlD_4$ in anhydrous diglyme according to a method from the patent literature.[21] For use as an LIF precursor, the reactive and unstable stannane was distilled into a Pyrex U-tube, cooled to −110 °C in an ethanol/liquid N_2 slush bath, and pressurized with 60 psi of argon.

A. *Ab initio* calculations

As a preliminary to exploratory experiments, we undertook a limited number of theoretical calculations of the properties of the ground ($\tilde{X}^1A_1$) and first excited singlet ($\tilde{A}^1B_1$) and triplet ($\tilde{a}^3B_1$) states of tin dihydride. First, we performed a series of density functional theory (DFT) calculations using the GAUSSIAN 09 program suite[22] with the Becke three-parameter hybrid density functional,[23] the Lee, Yang, and Parr correlation functional[24] (B3LYP), and Dunning's correlation consistent basis sets[25] augmented by diffuse functions (aug-cc-pVTZ). For the tin atom, an effective core potential (ECP) approach was adopted, using the aug-cc-pVTZ-pp basis set.[26] The geometric parameters of the three states were optimized, and the vibrational frequencies were calculated. In addition, higher level coupled cluster singles and doubles with triples added perturbatively [CCSD(T)] molecular structure and excitation energy calculations were also performed.

The results of our theoretical studies are summarized in Table I. In accord with all previous calculations, we find that tin dihydride is a nonlinear asymmetric top in all three states. With a bent molecular structure of C_{2v} symmetry, there are

TABLE I. *Ab initio* predictions [CCSD(T) with B3LYP in parentheses][a] of the ground and first two excited states of tin dihydride. All quantities are in cm^{-1} except where noted.

	$\tilde{X}^1A_1$		$\tilde{a}^3B_1$		$\tilde{A}^1B_1$	
	SnH_2	SnD_2	SnH_2	SnD_2	SnH_2	SnD_2
r(SnH) (Å)	1.757(1.783)	...	1.700(1.731)	...	1.699(1.738)	...
θ(HSnH) (deg)	91.1(90.4)	...	119.1(119.1)	...	119.6(119.9)	...
T_0	0	0	8951(10 489)	8931(10 493)	11 236(12 318)	11 215(12 335)
T_0 (SAC-CI)	0	0	...	...	15 442[b]	15 459[b]
ω_1	1780(1719)	1264(1221)	1886(1720)	1337(1219)	1 884(1673)	1 335(1185)
ω_2	805(781)	572(555)	678(664)	483(473)	677(656)	482(467)
ω_3	1784(1721)	1267(1222)	1946(1812)	1385(1290)	1 958(1778)	1 393(1266)

[a]All calculations with an aug-cc-pVTZ-pp basis set.
[b]Vibrational frequencies from B3LYP calculations.

two vibrations of a_1 symmetry denoted ν_1 (Si–H symmetric stretch) and ν_2 (bend) and a b_2 mode which is labeled ν_3 (Si–H antisymmetric stretch). The b axis bisects the H–Sn–H bond angle and I_c is out of the molecular plane. The ground state molecular orbital configuration is

$$\ldots.(b_2)^2(a_1)^2(b_1)^0 \quad \left(\tilde{X}^1A_1\right),$$

where the b_2 orbital is Sn–H σ bonding, the σ a_1 orbital is predominantly a 5*s* orbital on the tin atom, and the unoccupied π b_1 orbital is a tin out-of-plane 5*p* orbital. Promotion of an electron from the a_1 to the b_1 orbital yields $^{1,3}B_1$ excited states whose bond angle is substantially larger in accord with the predictions of Walsh diagrams.

Our CCSD(T)/DFT calculations predict that the 0-0 band of SnH_2 should occur at ~11 200/12 300 cm^{-1}. Both of these values are considerably smaller than the ~17 000 cm^{-1} CAS SCF/CI prediction published[13] in 1986. Similar calculations on SiH_2 and GeH_2 show that the CCSD(T)/DFT calculations seriously underestimate the electronic excitation energies (but not the geometries or vibrational frequencies) of the heavy-atom carbenes[27] due to the well-known multiconfigurational character of the ground states. To remedy this deficiency, we also used the symmetry adapted cluster-configuration interaction (SAC-CI) method implemented in GAUSSIAN 09 to obtain a better prediction. The geometries of the ground and first excited $^1B_1$ states were optimized (results very similar to the B3LYP values in Table I), and the difference of the energies was used to predict T_e. These were corrected to T_0 values using the DFT vibrational frequencies, with the results given in Table I.

Our best theoretical estimate (SAC-CI) of the location of the $\tilde{A}^1B_1$–$\tilde{X}^1A_1$ 0-0 band of $^{120}SnH_2$ is 15 442 cm^{-1}. The large increase in bond angle (~30°) on electronic excitation mandates that the absorption band system should consist of an extensive progression in the excited state bending frequency of ~650 cm^{-1}.

III. RESULTS AND ANALYSIS

A. LIF spectra

Exploratory LIF experiments using the commercially available tetramethyltin precursor showed a set of weak atomic-like lines near the blue edge of the DCM dye region, along with a system of other, as yet unidentified, bands, as shown in Fig. 1. The set of lines was so similar to the spectra of the corresponding SiH_2 and GeH_2 species[10,11] that we suspected almost immediately that they were due to SnH_2. Since there were no further similar sets of lines to lower energy, we assign the band in the 15 810–15 880 cm^{-1} region as the 0-0 band, in reasonable agreement with our 15 442 cm^{-1} prediction from the SAC-CI/DFT frequency calculations (Table I).

In an attempt to increase the LIF signal intensity and eliminate the impurity bands, we synthesized stannane (SnH_4), fulfilling both aims, as is also shown in Fig. 1. Deuterated stannane (see Fig. 1) gave a similar spectrum with a modest isotope shift (+26.9 cm^{-1}), as expected from our *ab initio* results, and more rotational lines, as might be anticipated from the smaller rotational constants, and the comparison of SiD_2 and GeD_2.[28,29]

As we scanned our LIF excitation laser to higher energy, four phenomena were observed, as illustrated in Fig. 2. First, a series of approximately equally spaced bands with an interval of 634/454 cm^{-1} were found, entirely consistent with assigning them as the excited state bending progression of SnH_2/SnD_2. Second, the number of rotational lines found in each band

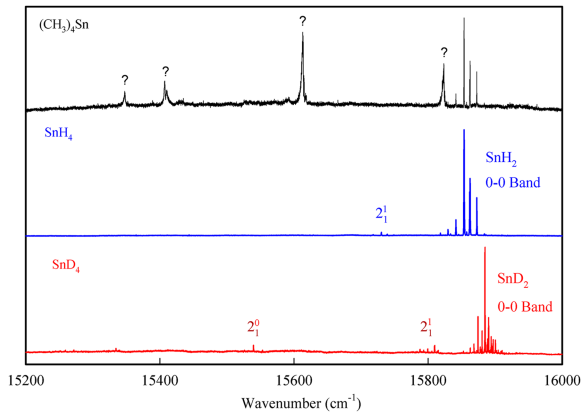

FIG. 1. Low resolution LIF spectra of tin dihydride in the DCM laser dye region. The top spectrum is that obtained using a tetramethyltin/argon precursor mixture. The bands marked ? are as yet unassigned. The middle spectrum is that obtained using a SnH_4/argon precursor. It shows a very strong SnH_2 0-0 band and a weaker 2^1_1 sequence band. The bottom spectrum is that recorded using SnD_4/argon and exhibits the $SnD_4$0-0 band, a weaker 2^1_1 band, and a weaker 2^0_1 hot band.

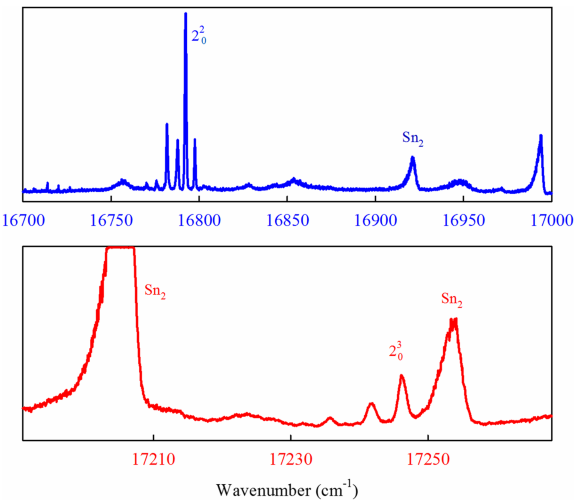

FIG. 2. LIF spectra of the 2_0^2 (top) and 2_0^3 (bottom) bands of SnD_2. The spectra are overlapped by bands of Sn_2 which get stronger to higher energy.

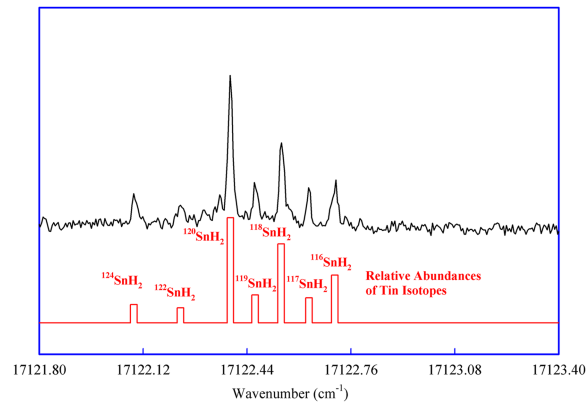

FIG. 3. The $^pP_1(1)$ line of the 2_0^2 band of SnH_2 (top) recorded at a resolution of 0.03 cm^{-1}. The relative abundances of the various tin isotopes are shown in the bar graph at the bottom.

decreased with increasing energy, as shown for the 2_0^2 and 2_0^3 bands of SnD_2 in Fig. 2. Third, the individual rotational lines showed significant broadening as is also evident in Fig. 2. Fourth, a very strong series of diatomic tin bands, identified by their hydrogen isotope independent ~188 cm^{-1} vibrational frequency in emission spectra,[30] grow in, making it difficult to follow the course of the stannylene bands at higher wavenumbers. The observed LIF band positions and assignments are summarized in Table II.

To prove conclusively that the new spectrum which we have ascribed to SnH_2 comes from a tin-containing molecule, we scanned some of the strongest lines in the LIF spectrum at high resolution, hoping to resolve some of the tin isotopologues. Tin has 10 naturally occurring isotopes of which 7 have abundances greater than 4%, with the most prominent being ^{120}Sn = 32.6% and ^{118}Sn = 24.2%. As shown in Fig. 3, the strongest feature of the 2_0^2 band of SnH_2 exhibits precisely the expected isotopic pattern. In lower bands, the individual transitions of the various tin isotopes overlap and are not completely resolved at 0.03 cm^{-1} resolution.

Returning now to the 0-0 band of SnH_2, we show it in detail in Fig. 4. The paucity of rotational lines immediately led us to suspect that SnH_2, like SiH_2 and GeH_2, undergoes a rotational-level-dependent predissociation in the excited state. Thus, we might expect that the transitions observed by LIF would be to the very lowest rotational levels in v′ =0 and that higher levels would have much reduced fluorescence lifetimes and quantum yields of fluorescence. Using the rotational constants derived from our *ab initio* structures, we simulated the expected rotational structure of the band at a typical temperature of 10 K, assuming that only transitions to $K_a' = 0$ would be prominent. As shown in Fig. 4, the comparison to the experiment is highly satisfactory, further confirming that SnH_2 is the carrier of the spectrum. It is important to emphasize that Boltzmann considerations would suggest that transitions from $K_a'' = 0$ to $K_a' = 1$ levels would be expected to be the strongest in the spectrum, but no such transitions are observed, strengthening our hypothesis of an excited state rotationally mediated predissociation process.

Although the 0-0 band LIF spectrum of SnH_2 does not contain enough information to derive a molecular structure, it is fortunate that the spectrum of SnD_2, shown in Fig. 5, is much richer. Starting again with the *ab initio* geometries, we calculated the rotational constants and simulated the spectrum, which allowed us to make a set of initial assignments

TABLE II. Assignments[a] of observed bands in the LIF spectra of SnH_2 and SnD_2.

Assign.	SnH_2 $^pP_1(1)$ (cm^{-1})	SnD_2 $^pP_1(1)$ (cm^{-1})
2_1^0	...	15 330.1
2_1^1	15 730.3	15 805.6
0_0^0	15 853.66[b]	15 880.62
2_0^1	16 487.8	16 334.2
2_1^3	...	16 691.7
2_0^2	17 122.4	16 787.8
2_0^3	17 758.0?	17 241.7
2_0^4	...	17 696.0?

[a]A very weak band at 17 011.4 cm^{-1} (SnD_2?) remains unassigned.
[b]The other measured line frequencies (cm^{-1}) and assignments for the 0-0 band of SnH_2 are $^pP_1(2)$ = 15 841.52, $^pP_1(3)$ = 15 829.68, $^pP_1(4)$ = 15 818.47, $^pQ_1(1)$ = 15 862.60, $^pQ_1(2)$ = 15 861.99, and $^pR_1(1)$ = 15 872.70.

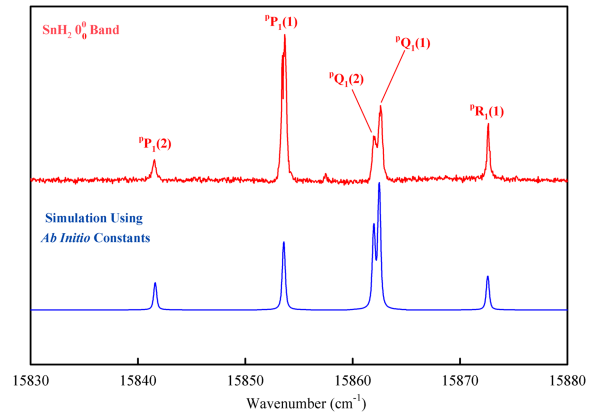

FIG. 4. The rotationally resolved LIF spectrum of the 0-0 band of SnH_2 (top) and the calculated spectrum (bottom) using the rotational constants calculated from the DFT *ab initio* structure. Only transitions to the upper state $K_a' = 0$ levels were included in the calculation, with a rotational temperature of 10 K. The band origin was adjusted to match the experimental results.

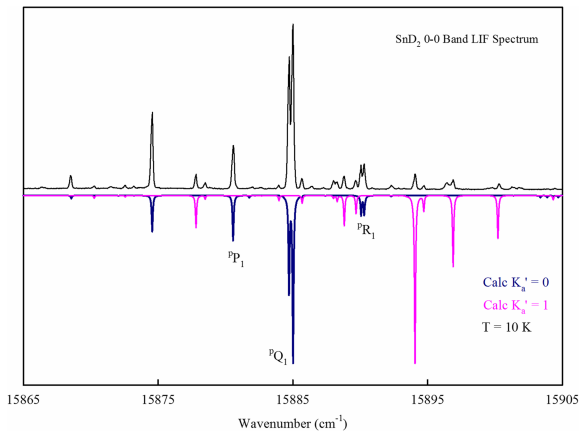

FIG. 5. The LIF spectrum of the 0-0 band of SnD_2 (top). The bottom spectrum is that calculated using the rotational constants in Table IV with a rotational temperature of 10 K. The stronger calculated transitions to $K'_a = 0$ are shown in blue, and the weaker transitions to $K'_a = 1$ are given in pink.

of the strong transitions to $K'_a = 0$. Bootstrapping up, we used our ASYROTWIN program[31] to fit the data and make further assignments of the weaker lines. In this way, a total of 39 transitions were fitted to an overall standard deviation of 0.014 cm^{-1}, varying the rotational constants in the upper and lower states and the band origin. The assignments are given in Table III, and the resulting constants are summarized in Table IV. Using these constants, we have calculated the rotational structure of the 0-0 band of SnD_2 at a temperature of 10 K, as shown in Fig. 5. Although the line positions are accurately reproduced, the intensities of the transitions to $K'_a = 1$ levels are calculated to be much stronger than observed, due to the predissociation process.

TABLE IV. The ground ($\tilde{X}^1A_1$) and excited state ($\tilde{A}^1B_1$) molecular constants of SnD_2 (in cm^{-1}).[a]

	$\tilde{X}^1A_1$	$\tilde{A}^1B_1$
A	2.8307(59)	6.3428(54)
B	2.6363(38)	1.8179(17)
C	1.3519(22)	1.3905(27)
T_0	0	15 886.093(15)

[a]The numbers in parentheses are standard errors of 3σ.

B. Emission spectra

Emission spectra, recorded in segments of ~800 cm^{-1} with our gated CCD detector, were studied for a variety of laser excitation wavelengths for both SnH_2 and SnD_2. Some examples are shown in Fig. 6. The extent of the spectra is limited by the 730 nm cutoff wavelength of the CCD detector. Despite this limitation, it is evident that the emission spectrum of SnH_2 is dominated by a long progression in the bending mode (ν_2 fundamental = 770 cm^{-1}, *ab initio* B3LYP = 781 cm^{-1}), as expected for a transition involving an almost 30° change in the bond angle. A weak transition down to ν''_1 is also observed (ν_1 = 1679 cm^{-1}, *ab initio* B3LYP = 1719 cm^{-1}) as the beginning of a minor stretch-bend progression. The SnD_2 emission spectrum is very similar but extends to $\nu''_2 = 6$ due to the smaller bending frequency and yields ν_2 = 549 and ν_1 = 1204 cm^{-1} compared to *ab initio* B3LYP values of 555 and 1221 cm^{-1}.

TABLE III. Rotational line frequencies (cm^{-1}) and assignments for the 0-0 band of SnD_2.

	$K'_a = 1 - K''_a = 0$ subband			$K'_a = 0 - K''_a = 1$ subband		
J'	$^rR_0$	$^rQ_0$	J'	$^pR_1$	$^pQ_1$	$^pP_1$
1	15 894.275(22)[a,b]	15 889.838(0)	0			15 880.619(−7)
2	15 897.105(−4)	15 888.964(3)	1		15 885.115(−3)	15 874.548(−25)
3	15 900.510(19)	15 888.407(−21)	2	15 890.226(4)	15 884.814(0)	15 868.528(14)
4	15 904.624(6)	15 888.184(25)	3	15 890.468(−4)	*15 884.814(−30)	15 863.038(15)
5	15 909.394(0)	...	4	*15 890.468(−110)	*15 885.115(−89)	15 857.934(19)
			5	15 891.082(6)	15 885.788(−20)	15 853.051(−6)
	$K'_a = 2 - K''_a = 1$ subband			$K'_a = 1 - K''_a = 2$ subband		
J'	$^rR_1$	$^rQ_1$	J'	$^pR_2$	$^pQ_2$	$^pP_2$
2	15 909.226(−8)	15 899.944(0)	1			15 877.819(−13)
	15 910.492(3)					15 878.522(7)
3	15 909.715(2)		2		...	15 870.254(7)
	15 913.407(−16)				15 885.788(2)	15 872.538(−2)
4	*15 910.492(134)		3	15 894.930(7)	...	15 862.490(12)
	15 916.776(23)			15 893.470(−1)	15 884.038(−31)	15 866.582(−14)
5	...		4	*15 894.275(154)		
	15 920.532(−6)			*15 893.470(39)		
6	...		5	15 893.065(−11)		
	...			...		

[a]The numbers in parentheses are observed minus calculated values in units of 10^{-3} cm^{-1}. An asterisk denotes a blended line not used in the least squares fit. In cases where the asymmetry doubling is resolved, the transition with even parity ($J + K_a + K_c$) in the lower state is listed first.

[b]Lines at 15 852.793, 15 862.806, and 15 873.192 cm^{-1} could plausibly be assigned as $3_{0,3}$-$4_{3,1}$, $2_{0,2}$-$3_{3,0}$, and $3_{0,3}$-$3_{3,1}$ respectively, but they did not fit very well and were omitted from the least squares analysis.

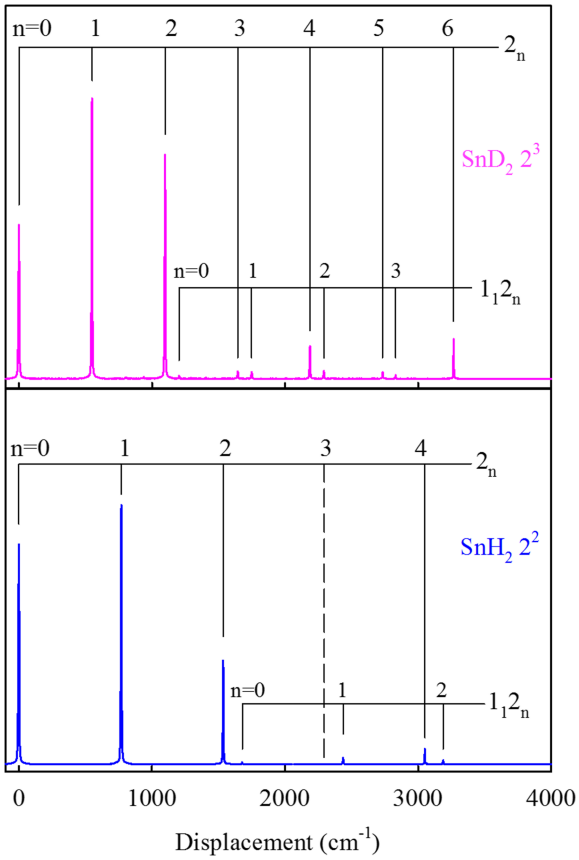

FIG. 6. Emission spectra of SnD_2 (top) obtained by pumping the $^pP_1(1)$ line of the 2_0^3 band and SnH_2 (bottom) by laser excitation of the 2_0^2 band $^pP_1(1)$ line. In each case, the horizontal axis is the displacement from the laser wavenumber, giving a direct measure of the ground state energy of each transition.

Clearly, the emission data, summarized in Table V, are entirely consistent with our assignment of the spectra as due to the SnH_2/SnD_2 molecules.

C. Fluorescence lifetimes

Figure 7 shows the fluorescence decay curves and lifetimes of the three lowest rotational levels of the zero-point vibrational level of the excited state of SnH_2. In all cases,

TABLE V. Ground state energy intervals[a] (in cm^{-1}) and their assignments from the $^pP_1(1)$ emission spectra of SnH_2 and SnD_2.

Assignment[b]	SnH_2	SnD_2
2_1	770	549
2_2	1535	1098
1_1	1679	1204
2_3	2295	1643
$1_1 2_1$	2437	1749
2_4	3052	2188
$1_1 2_2$	3188	2291
2_5	...	2730
$1_1 2_3$	...	2831
2_6	...	3267

[a]Energy above the v″ = 0, $1_{1,0}$ rovibronic level of the ground electronic state.
[b]In each case, the rotational level in the vibrationally excited state is $1_{1,0}$ ($J_{Ka,Kc}$).

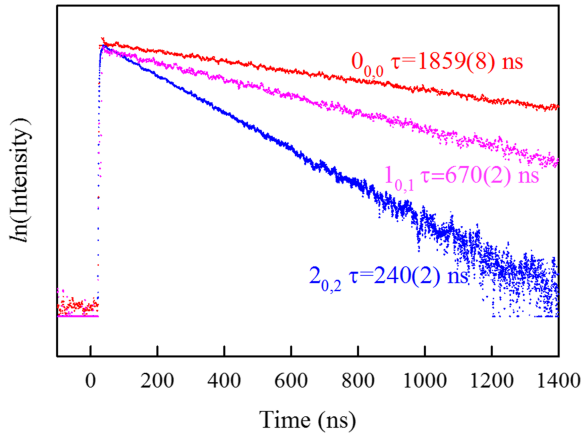

FIG. 7. Fluorescence decay curves [plotted as ln(intensity) versus time] for the three lowest rotational levels in the vibrationless level of the $\tilde{A}^1B_1$ state of SnH_2. The fluorescence lifetime obtained from each decay curve is also given.

good single exponential decays were observed over 2-3 lifetimes. The $0_{0,0}$ ($J_{Ka,Kc}$) level has a lifetime of 1.86(1) μs, which we take as the radiative lifetime, comparable to the value of 1.1 ± 0.11 μs measured[10] for SiH_2. A very slight increase in rotational energy to the level $1_{0,1}$ diminishes the SnH_2 lifetime by a factor of three and $2_{0,2}$ has a decay rate 7.7 times faster than $0_{0,0}$. Since the $^pP_1(1)$ lines (upper state $0_{0,0}$) show up strongly for the 2_0^1, 2_0^2, and 2_0^3 bands, they must also have substantial lifetimes, whereas the degradation of rotational structure in these higher bands points to rapid lifetime diminution with rotational energy. The decay dynamics are obviously very strongly dependent on the rotational state within a given excited state vibronic level, very similar to the behavior observed in silylene and germylene.[10,11]

IV. DISCUSSION

A. The molecular structure of SnH_2

We have used the rotational constants determined from the 0-0 band LIF spectrum of SnD_2 to determine the molecular structure of tin dihydride. Planar moments ($P_{A,B,\text{ or }C}$) rather than the raw rotational constants or moments of inertia were used for the least squares analysis to minimize correlations between the geometric parameters. Since the out-of-plane planar moment P_C must by definition be zero, the data set included only P_A and P_B of SnD_2. The resulting structures are summarized in Table VI. The agreement between the experimental and *ab initio* values (Table I) is very good. In the ground state, the SnH_2 bond length is only ~0.013 Å shorter than that of the SnH free radical,[32] a trend that is found for the silylene and germylene species as well (see Table VI). By contrast, the stannylene bond length is some 0.057 Å longer than the bond length of stannane[33] (SnH_4) with similar results for silylene (+0.034 Å) and germylene (+0.068 Å). The longer SnH_2 bond length is entirely consistent with a SnH_2 symmetric stretching frequency of 1679 cm^{-1} (Table V) which is substantially smaller than the symmetric stretching frequency of stannane (ν_1 = 1907.8 cm^{-1}).[33]

As early as 1986, Balasubramanian[13] noted the remarkable similarity of the calculated properties of the electronic

TABLE VI. Comparison of the ground and excited state geometric parameters of SiH_2, GeH_2, and SnH_2.

Parameter	SiH_2	$^{74}GeH_2$	SnH_2
r'' (X–H) (Å)	1.514(1)[a]	1.5934(2)[b]	1.768(4)[c]
θ'' (deg)	91.98(4)	91.28(1)	91.0(3)
r'' XH diatomic (Å)[d]	1.5281	1.588	1.781
r' (X–H) (Å)	1.485(3)	1.5564(5)	1.729(5)
Δr (X–H) (Å)[e]	–0.029	–0.0370	–0.039
θ' (deg)	122.44(20)	123.02(2)	122.9(2)
$\Delta(\theta)$ (deg)[e]	30.46	31.74	31.9
T_0	15 547.7730(93)	16 324.5086(78)	15 886.09(2)

[a]Reference 36, approximate r_e structure, errors estimated from reference Table IV data.
[b]Reference 28, r_0 structure.
[c]This work (r_0 structures).
[d]Reference 32, r_e values.
[e]Change in geometric parameter on electronic excitation.

states of SnH_2 to those of SiH_2 and GeH_2. Table VI shows a comparison of the known experimental values for the heavy carbene analogs. The ground state bond lengths scale with the size of the central atom, and the bond angles are all very similar, decreasing very slightly down the group. The electronic excitation energies are all within 5% of each other although they involve different valence shell orbitals (3*s* and 3*p* for silylene, up to 5*s* and 5*p* for stannylene). In each case, the bond angle increases by 30°–31° on electronic excitation, with a slight trend toward a larger increase down the group. By contrast, the bond lengths all decrease by about 0.03 Å on electronic excitation.

B. Predissociation

All experimental indications (LIF spectra, fluorescence lifetimes, and linewidths) are that SnH_2 undergoes a rotational-level-dependent predissociation process in the excited state, similar to that in SiH_2 and GeH_2. In the case of the latter two molecules, the experimental and theoretical evidence suggests that the lower vibrational levels are predissociated leading to the products Si (^3P) + H_2. The exact mechanism of this process is up for debate. Obi and co-workers[10,28] have argued that the heterogeneous perturbation can be explained by the mechanism $\tilde{A}^1B_1$–(*a*-type Coriolis)–$\tilde{X}^1A_1$–(spin-orbit)–$\tilde{a}^3B_1 \rightarrow$ Si (^3P) + H_2. Others have suggested alternate pathways although the fine details are not well understood.[34,35] Experimentally, there appears to be clear evidence of a barrier to dissociation[28] based on the rotational structure in the LIF spectra of SiH_2 and SiD_2. For germanium dihydride, our own theoretical calculations predict a similar barrier to dissociation from the $\tilde{a}^3B_1$ state.[11]

At higher vibrational energies in the excited state, both SiH_2 and GeH_2 show evidence of a second dissociation channel which leads to a complete breaking off of fluorescence. Calculations indicate that this is the onset of the formation of excited state atoms (^1D) and ground state hydrogen molecules. Unfortunately, our SnH_2 spectra are so badly overlapped by strong Sn_2 bands that we cannot at present determine if there is a similar abrupt termination of the fluorescence for higher vibrational levels in the $\tilde{A}$ state. Perhaps in future, experimental methods will be devised to produce SnH_2 without the diatomic tin products, which would help explore this point.

It seems most likely that the excited state dynamics of SnH_2 are very similar to the corresponding processes in silylene and germylene. At low vibrational energies, a rotationally mediated process leads to a predissociation producing an atom and a hydrogen molecule. This process is strongly affected by deuteration, which results in more extensive rotational structure in the LIF spectra of the deuterated species. The fluorescence lifetimes decrease very rapidly with total rotational angular momentum, even within the K'_a= 0 stack of levels. High level *ab initio* studies including the effects of spin-orbit coupling would be useful to see if the manifold of states, dissociation limits, and transition states of tin dihydride are similar to those of SiH_2 and GeH_2.

V. CONCLUSIONS

The tin dihydride molecule has been conclusively identified in the gas phase. The LIF and emission spectra of SnH_2 and SnD_2 have been studied in some detail, and the ground and excited state vibrational frequencies, rotational constants, observed tin isotope splittings, and hydrogen/deuterium isotope effects are entirely consistent with expectations for tin dihydride. The rotational structure in the 0-0 band of SnD_2 has been analyzed and the molecular structure derived yielding a ground state bond length of 1.768 ± 0.004 Å and a bond angle of 91.0° ± 0.3°. The bond angle increases by 31.9° and the bond length decreases by 0.039 Å on electronic excitation, trends predicted by our calculations at the CCSD(T) and B3LYP levels of theory. The limited rotational structure and intensity anomalies in the LIF spectra indicate that SnH_2/SnD_2 undergoes a rotational-level-dependent predissociation process in the $\tilde{A}^1B_1$ state.

ACKNOWLEDGMENTS

D.J.C. is very grateful to the staff of Ideal Vacuum Products LLC for making his sabbatical leave in Albuquerque in the spring of 2017 such an enjoyable and productive time. This research was funded by Ideal Vacuum Products.

[1]A. Orita and J. Otera, *Main Group Metals in Organic Synthesis*, edited by H. Yamamoto and K. Oshima (John Wiley and Sons, 2004), Vol. 2, pp. 621–720.
[2]W. P. Neumann, J. Organomet. Chem. **437**, 23 (1992).
[3]M. D. Allendorf and A. M. B. van Mol, Top. Organomet Chem. **9**, 1 (2005).
[4]A. M. B. van Mol, Y. Chase, A. H. McDaniel, and M. D. Allendorf, Thin Solid Films **502**, 72 (2006).
[5]C. L. Senaratne, J. D. Gallagher, L. Jiang, T. Aoki, D. J. Smith, J. Menendez, and J. Kouvetakis, J. Appl. Phys. **116**, 133509 (2014).
[6]J. Xie, A. V. G. Chizmeshya, J. Tolle, V. R. D'Costa, J. Menendez, and J. Kouvetakis, Chem. Mater. **22**, 3779 (2010).
[7]T. Krenek, P. Bezdicka, N. Murafa, J. Subrt, and J. Pola, Eur. J. Inorg. Chem. **2009**, 1464.
[8]P. R. Bunker, P. Jensen, W. P. Kraemer, and R. Beardsworth, J. Chem. Phys. **85**, 3724 (1986).
[9]J. E. Rice and N. C. Handy, Chem. Phys. Lett. **107**, 365 (1984).
[10]M. Fukushima, S. Mayama, and K. Obi, J. Chem. Phys. **96**, 44 (1992).
[11]J. Karolczak, W. W. Harper, R. S. Grev, and D. J. Clouthier, J. Chem. Phys. **103**, 2839 (1995).
[12]X. Wang, L. Andrews, G. V. Chertihin, and P. F. Souter, J. Phys. Chem. A **106**, 6302 (2002).
[13]K. Balasubramanian, Chem. Phys. Lett. **127**, 585 (1986).

[14]Z. Barandianin and L. Seijo, J. Chem. Phys. **101**, 4049 (1994).
[15]T. Mineva, N. Russo, E. Sicilia, and M. Toscano, Int. J. Quantum Chem. **56**, 669 (1995).
[16]N. Matsunaga, S. Koseki, and M. S. Gordon, J. Chem. Phys. **104**, 7988 (1996).
[17]H. Harjanto, W. W. Harper, and D. J. Clouthier, J. Chem. Phys. **105**, 10189 (1996).
[18]W. W. Harper and D. J. Clouthier, J. Chem. Phys. **106**, 9461 (1997).
[19]D. L. Michalopoulos, M. E. Geusic, P. R. R. Langridge-Smith, and R. E. Smalley, J. Chem. Phys. **80**, 3556 (1984).
[20]S. Gerstenkorn and P. Luc, *Atlas du Spectre D'Absorption de la Molecule d'Iode* (Editions du CNRS, Paris, 1978); Rev. Phys. Appl. **14**, 791 (1979).
[21]Cole J. Ritter III, "Synthesis of stannane and deuterostannane," U.S. patent 20130129607 A1 (May 23, 2013).
[22]M. J. Frisch, G. W. Trucks, H. B. Schlegel *et al.*, GAUSSIAN 09, Revision A.02, Gaussian, Inc., Wallingford, CT, 2004.
[23]A. D. Becke, J. Chem. Phys. **98**, 5648 (1993).
[24]C. Lee, W. Yang, and R. G. Parr, Phy. Rev. B **37**, 785 (1988).
[25]T. H. Dunning, Jr., J. Chem. Phys. **90**, 1007 (1989).
[26]K. A. Peterson, J. Chem. Phys. **119**, 11099 (2003).
[27]D. J. Clouthier (unpublished).
[28]M. Fukushima and K. Obi, J. Chem. Phys. **100**, 6221 (1994).
[29]T. C. Smith, D. J. Clouthier, W. Sha, and A. G. Adam, J. Chem. Phys. **113**, 9567 (2000).
[30]V. E. Bondybey, M. Heaven, and T. A. Miller, J. Chem. Phys. **78**, 3593 (1983).
[31]R. H. Judge and D. J. Clouthier, Comput. Phys. Commun. **135**, 293 (2001).
[32]K. P. Huber and G. Herzberg, *Constants of Diatomic Molecules* (Van Nostrand Reinhold, New York, 1979).
[33]H. W. Kattenberg and A. Oskam, J. Mol. Spectrosc. **51**, 377 (1974).
[34]J. S. Francisco, R. Barnes, and J. W. Thoman, Jr., J. Chem. Phys. **88**, 2334 (1988).
[35]G. Duxbury, A. Alijah, and R. R. Trieling, J. Chem. Phys. **98**, 811 (1993).
[36]R. Escribano and A. Campargue, J. Chem. Phys. **108**, 6249 (1998).